OPEN ACCESS

Scholars International Journal of Chemistry and Material Sciences

Abbreviated Key Title: Sch Int J Chem Mater Sci
ISSN 2616-8669 (Print) |ISSN 2617-6556 (Online)
Scholars Middle East Publishers, Dubai, United Arab Emirates
Journal homepage: http://saudijournals.com/sijcms/

Original Research Article

Synthesis and Ab Initio Determination $Bi_{1.256}$ $La_{0.53}$ $N_{0.231}$ $O_{0.521}$ $Zr_{1.543}$ Triclinic Structure from Powder X-Ray Diffraction Data

Bimal K. Kanth, Parashuram Mishra*

Bioinorganic, Materials Chemistry Research Lab. Tribhuvan University, M.M.A.M. Campus, Biratnagar, Nepal

DOI: 10.36348/sijcms.2020.v03i06.002 | **Received:** 18.07.2020 | **Accepted:** 25.07.2020 | **Published:** 09.08.2020

***Corresponding author:** Parashuram Mishra

Abstract

This paper is examined the synthesis and ab initio structure determination of the heavy metal framework mixed valence $Bi_{1.256}$ $La_{0.53}$ $N_{0.231}$ $O_{0.521}$ $Zr_{1.543}$from precession electron diffraction intensities The metal framework of the compound was solved in this investigation via direct methods from Powder XRD.A subsequent (kinematical) least-squares refinement with electron intensities yielded slightly improved co-ordinates for the 6 heavy atoms in the structure. Chemical analysis of several crystallites by EDX is in agreement with the formula $Bi_{1.256}$ $La_{0.53}$ $N_{0.231}$ $O_{0.521}$ $Zr_{1.543}$ Moreover, the structure was independently determined by Rietveld refinement from X-ray powder data obtained from a multi-phasic sample. The compound having triclinic crystal system space group P-1 and Centrosymmetry structure with refined lattice parameters a=5.8655, b=4.4099, c=17.6031, α =82.0712, β =88.251 and γ =74.4651 Comparison of the framework structure from electron diffraction with the result from Rietveld refinement shows an average agreement for the heavy atoms within 0.09A˚. The titled compound was prepared from mixture of Bi_2O_3 –$Zr(NO_3)_4$ and La_2O_3 by solid state reaction with full thermal decomposition at 1000°C. Rwp = 0.0680, Rp = 0.030 and GOF=0.31 and the structure factors F0 = 2023 and Fc = 2021.

Keywords: Centrosymmetry, X-ray diffraction, EDX, multi-phase, refinement.

INTRODUCTION

A recent investigation of structural and conductivity properties of $Bi_{1.256}$ $La_{0.53}$ $N_{0.231}$ $O_{0.521}$ $Zr_{1.543}$ oxide and nitride conductors (*Bi, La and Zr)* which belong to the dimorphic tri clinic structural-type family, has proved a close conductivity composition dependence [1]. This has been interpreted on the basis of structural data obtained from Rietveld structure refinements based on previous crystal structure investigations [2]. The structure is built from cationic slabs parallel to (001) faces of the triclinic cells. N and two oxygen sites are located inside; complementary oxide ions, implied by the formulation stoichiometries, are distributed over one or two sites of the inters lab space and exhibit a high mobility, mainly responsible for the conductivity [3]. Depending on the rare-earth nature, at high-temperature form is observed, with a closely hexagonal related structure; its formation from the b2 low-temperature variety occurs during a phase transition that has been attributed to a cationic disordering in the mixed Bi3`/¸*n*3` layers [3]. It is accompanied by sudden increases of both lattice parameters, of oxide occupancy in inter slab spaces, and of the conductivity. The pure iron oxide conductor character of the variety has been clearly demonstrated for the alkaline-earth-based solid solutions and has been also verified for lanthanides-based solid solutions (unpublished results).The thickness of the cationic slabs, which is the largest for the lanthanum term $Bi_{1.256}$ $La_{0.53}$ $N_{0.231}$ $O_{0.521}$ $Zr_{1.543}$ (the best oxide conductor ever evidenced in this family: [4] with *E*!="0.8 eV), appears to be an important factor for these attractive conductivity properties. $Bi_{1.256}$ $La_{0.53}$ $N_{0.231}$ $O_{0.521}$ $Zr_{1.543}$a term of a wide Bi1~*x*La*x*O1.5 solid solution domain, with 0.154*x*40.333, which exhibits anomalies in the evolution of the cell parameters versus composition [5] for one of the particular compositions & $Bi_{17}La_4O_{31.5}$ and ZrN," which is identical to $Bi_{1.256}$ $La_{0.53}$ $N_{0.231}$ $O_{0.521}$ $Zr_{1.543}$, a thermal investigation of the quenched to high-temperature form led to evidence of a triclinic crystal system. This paper deals with the *ab initio* structure determination of this new phase from powder X-ray diffraction data; identification and investigation of the corresponding solid solution, using various techniques such as X-ray diffraction method.

MATERIAL AND METHOD

All chemicals used were analytical grade. A polycrystalline sample of $Bi_{1.256}$ $La_{0.53}$ $N_{0.231}$ $O_{0.521}$ $Zr_{1.543}$ was synthesized by a standard solid state reaction using a mixture of high purity reagents of Bi_2O_3, $Zr(NO_3)_4$ and La_2O_3 which contained mixed valence as the starting materials in the molar ratio of 1: 1: 1. The mixture was ground carefully, homogenized thoroughly with methanol (99%) in an agate mortar pestle and then packed into an alumina crucible and calcined at 1000°C in air for 30h with several intermediate grindings [6]. Finally the product was pressed into pallets and sintered at 100 K/h. Powder X-ray diffraction (XRD) data were collected at room temperature in the angular range of 2θ =10 to 90 with scan step width of 0.02° and a fixed containing time of 15 s using Philips powder diffractometer with graphite monochromatic CuKa radiation. The powder was rotated during the data collection to minimize preferred Orientation effect if any. The program TREOR in CRYSFIRE was used to index the powder pattern which give triclinic cell system.SIRPOW92 was used to locate the positional parameters of constituent atoms. The full pattern is fitting and peak decomposition in the space group P-1 using check cell program. The structural parameters were refined by the Rietveld method using the JANA program which gave at 1000°C. Rwp = 0.0680, Rp = 0.030 and GOF=0.31 and the structure factors F0 = 2023 and Fc = 2021. . The density is determined by Archimedes principle.

RESULTS AND DISCUSSIONS

The crystal structure of $Bi_{1.256}$ $La_{0.53}$ $N_{0.231}$ $O_{0.521}$ $Zr_{1.543}$ is as shown in figure 7. The zirconium occupies the MO6 position in the perovskite layer. However, the continuous O–La–O chains expected in a simple perovskite is disrupted at every n = 4 along the c axis by $[Bi2O2]^{2+}$ layers. The Zr–N distances range from 1×301(4) to 2×557Å with alternate bonds being long and short to result in a zigzag arrangement of ZrO_3^{-2} octahedra [7]. The range of the Zr- N and La–O distances calculated appear to be rather large than those reported in the literature for similar systems. However, more accurate bond lengths have been obtained via neutron diffraction studies for $Bi_{1.256}$ $La_{0.53}$ $N_{0.231}$ $O_{0.521}$ $Zr_{1.543}$ [8]. The differences in ionic radii ofBi, La and Zr ions also appear to influence the tilt and distortion of the $ZrO3^{-2}$ octahedra. The Bi–O distances range from 2×25 Å to 3×31 Å. The structure $Bi_{1.256}$ $La_{0.53}$ $N_{0.231}$ $O_{0.521}$ $Zr_{1.543}$ has three Bi atoms in the asymmetric unit with one of the atoms [Bi(3)] forming the [Bi2O2]2+ layer, while the other two [Bi(1) and Bi(2)] belong to the perovskite layers. Bi (1) and Bi (2) are coordinated to 12 oxygen atoms and Bi(3) is coordinated to 8 oxygens. The structure of $Bi_{1.256}$ $La_{0.53}$ $N_{0.231}$ $O_{0.521}$ $Zr_{1.543}$is refined using the Rietveld method in the space group *P-1*. However, it is noteworthy that earlier reports [10] on thin films of this material demonstrate that it is ferroelectric when grown in specified directions. This suggests the possibility of centrosymmetric arrangements in specific domains in certain crystallographic directions. The occupancy refinements suggest that only in case of $Bi_{1.256}$ $La_{0.53}$ $N_{0.231}$ $O_{0.521}$ $Zr_{1.543}$ the Zr cations get localized in the Bi2O2 layers. However, it is hard to ascertain this feature since the scattering factors for X-rays for Bi and Zr are nearly the same. On the other hand, it is clear that in the other two compounds the Bi/Zr cations are distributed in both Bi2O2 and the perovskite layers. Table 2provides a list of valence bond sums [11] in all these three structures, which indicate a measure of the extent of disorder in these phases. It also compares the tendency of the three oxides to incorporate A type cations in the [Bi2O2] layer and the perovskite layers [12].

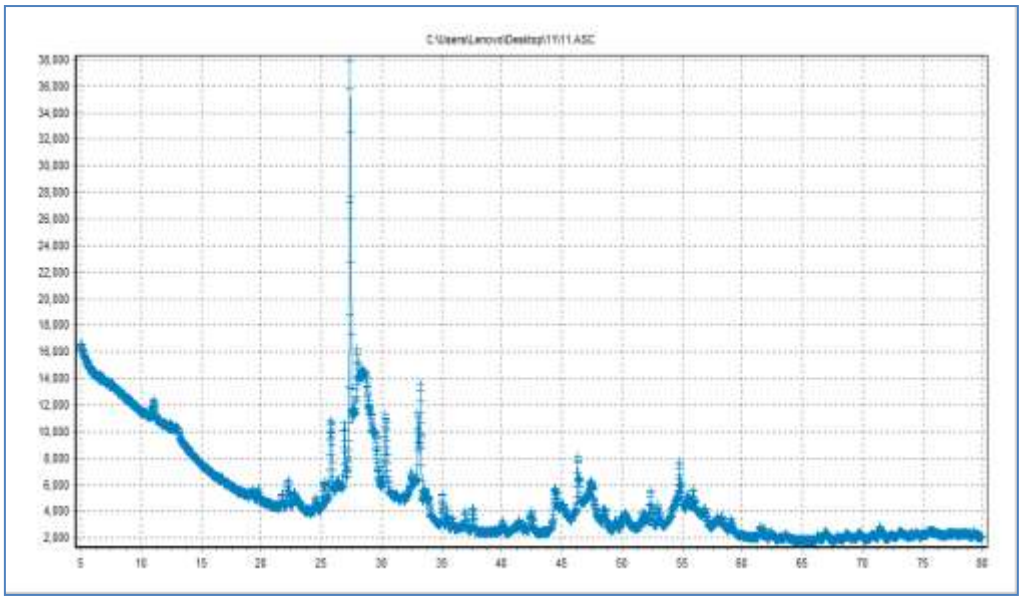

Fig-1: Powder XRD spectra of $Bi_{1.256}$ $La_{0.53}$ $N_{0.231}$ $O_{0.521}$ $Zr_{1.543}$

Crystal structures

High-resolution data set was collected for $Bi_{1.256}$ $La_{0.53}$ $N_{0.231}$ $O_{0.521}$ $Zr_{1.543}$ on a Philips powder diffractometer utilizing CuKαradiation. The refinement was done using the JANA2006 software. As in the case of $Bi_{1.256}$ $La_{0.53}$ $N_{0.231}$ $O_{0.521}$ $Zr_{1.543}$ [13-16], indexing the powder patters was not straightforward as two sets of Miller indices are possible for the strongest reflections yielding two alternative unit cells which led to close residuals upon LeBail full-pattern decomposition. Subsequent Rietveld refinements clearly ruled out one of these due to intolerably dissimilar La–O distances in the Bi_2O3^{-3} anion. Final Rietveld refinement plot for $Bi_{1.256}$ $La_{0.53}$ $N_{0.231}$ $O_{0.521}$ $Zr_{1.543}$43 is given in Figure. 3; general projection of the Perovskite crystal structure is shown in Figure 2; the refinement results are collected in Tables 1.For $Bi_{1.256}$ $La_{0.53}$ $N_{0.231}$ $O_{0.521}$ $Zr_{1.543}$structures was refined from routine XRD data to confirm the same atomic arrangement; these refinements also converged to reasonable R values. Just traces of by-products were present which could not be identified as their estimated content is below 1%.

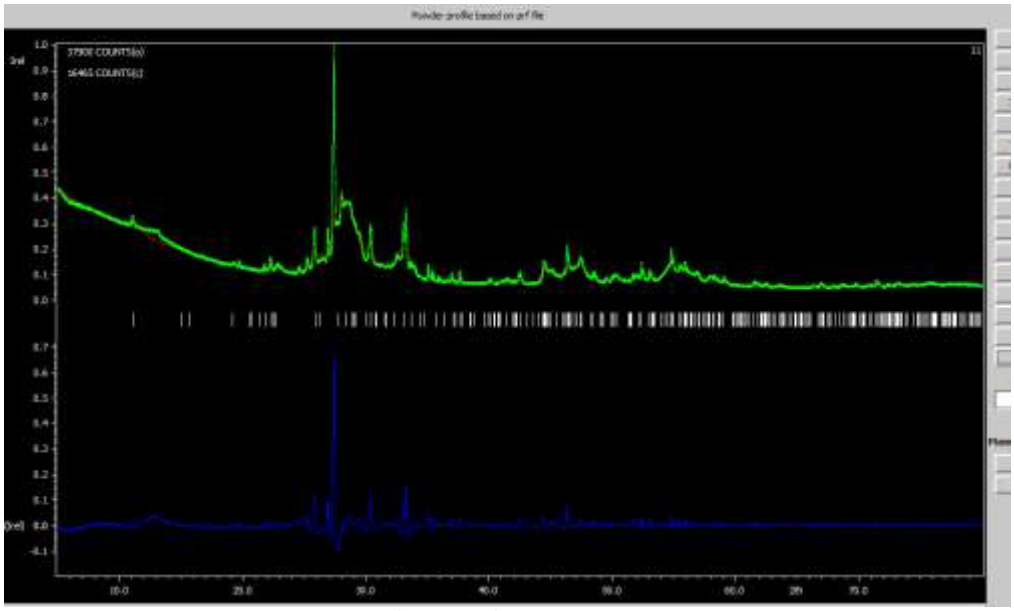

Fig-2: Rietveld refinement of Bi1.256 $La_{0.53}$ $N_{0.231}$ $O_{0.521}$ $Zr_{1.543}$

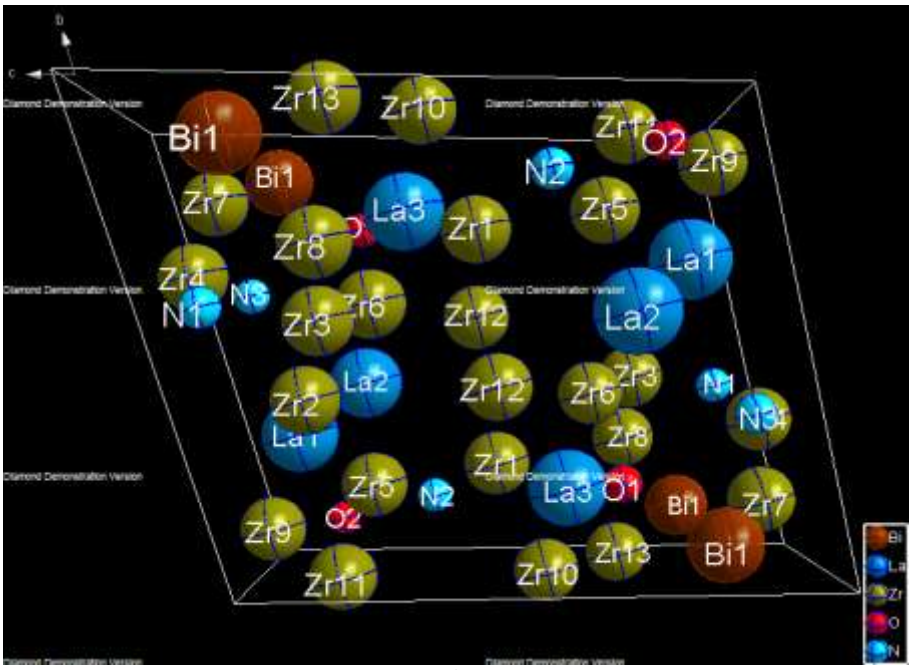

Fig-3: Perovskite structure of $Bi_{1.256}$ $La_{0.53}$ $N_{0.231}$ $O_{0.521}$ $Zr_{1.543}$

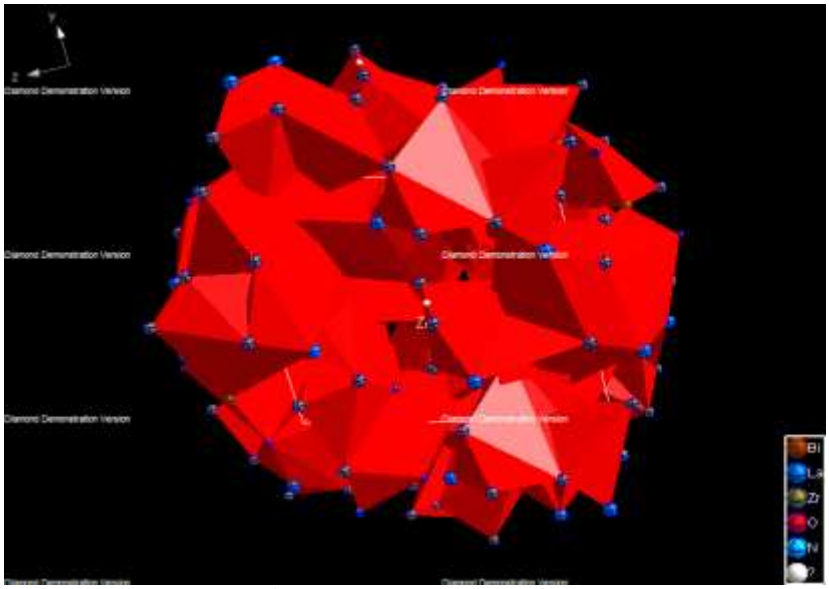

Fig-3: General projection of polyhedron type structure of $Bi_{1.256}$ $La_{0.53}$ $N_{0.231}$ $O_{0.521}$ $Zr_{1.543}$

Table-1: Crystallographic data after Rietveld refinement

Formula sum	$Bi_{1.256}$ $La_{0.53}$ $N_{0.231}$ $O_{0.521}$ $Zr_{1.543}$
Formula weight	488.4 g/mol
Crystal system	triclinic
Space-group	P -1 (2)
Cell parameters	a=5.0302 Å b=7.2625 Å c=8.3400 Å α=74.3014° β=84.4133° γ=74.2675°
Cell ratio	a/b=0.6926 b/c=0.8708 c/a=1.6580
Cell volume	282.23 $Å^3$
Z	2
Calc. density	5.74684 g/cm^3
Meas. density	5.7659g/cm^3
Pearson code	aP43
Formula type	N2O4P6Q6R25
Indexes	-1≤ h≤,2,0≤,k≤ 2,-1≤,l≤,3
Wyckoff sequence	i21f

Table-2: Fraction Atomic parameters

Atom	Ox.	Wyck.	Site	S.O.F.	x/a	y/b	z/c	U [$Å^2$]
Bi1	3	2i	1		-0.00536	0.10643	0.20272	0.0380
La1	3	2i	1		-0.66940	0.30889	0.87557	0.0380
La2	3	2i	1		-1.02512	0.57776	0.25235	0.0380
La3	3	2i	1		-0.41060	0.19881	0.42437	0.0380
Zr1	4	2i	1		-0.57773	0.24545	0.53666	0.0380
Zr2	4	2i	1		-0.71116	0.60189	0.18303	0.0380
Zr3	4	2i	1		-0.76396	0.43947	0.24622	0.0380
Zr4	4	2i	1		-0.52333	0.34626	0.04873	0.0380
Zr5	4	2i	1		-0.53518	0.20067	0.76182	0.0380
Zr6	4	2i	1		-0.67793	0.40350	0.33281	0.0380
Zr7	4	2i	1		-0.29135	0.17799	0.10042	0.0380
Zr8	4	2i	1		-0.87047	0.29054	0.28411	0.0380
Zr9	4	2i	1		-0.53782	0.10083	0.96235	0.0380
Zr10	4	1f	-1		-1/2	0	1/2	0.0380
Zr11	4	2i	1		0.30565	-0.01498	0.15334	0.0380
Zr12	4	2i	1		-0.31980	0.42431	0.49792	0.0380
Zr13	4	2i	1		0.23623	0.01199	0.35639	0.0380
O1	2	2i	1		-0.16966	0.22472	0.33583	0.0380
O2	2	2i	1		-0.11962	-0.09476	0.13916	0.0380
N1	3	2i	1		-0.88339	0.41703	0.08263	0.0380
N2	3	2i	1		-0.12394	-0.14891	0.32576	0.0380
N3	3	2i	1		-0.10011	0.37329	0.09634	0.0380

Table-3: Selected bond angles

Atom 1	Atom 2	Atom Code	Atom 3	Atom Code 2	Bond angle
Bi1	O1	18555011	Zr7	11555011	87.657
	O1	18555011	Zr11	15555011	142.246
	O1	18555011	Zr13	17555011	82.017
	O1	18555011	N3	22555011	71.966
	O1	18555011	O2	19555011	124.559
	O1	18555011	Zr8	12655011	55.503
	O1	18555011	N2	21555011	92.567
	O1	18555011	N1	20655011	81.950
	Zr7	11555011	Zr11	15555011	129.753
	Zr7	11555011	Zr13	17555011	164.067
	Zr7	11555011	N3	22555011	66.185
	N3	22555011	O2	19555011	125.363
	N3	22555011	Zr8	12655011	60.076
	N3	22555011	N2	21555011	149.571
	N3	22555011	N1	20655011	28.894
La1	Zr5	9555011	La2	3366021	92.393
	Zr5	9555011	O2	19456021	68.926
	Zr9	13555011	La2	3366021	132.607
	Zr9	13555011	O2	19456021	64.325
	Zr9	13555011	Zr2	6466021	95.447
	Zr9	13555011	N1	20556011	100.488
	Zr9	13555011	N3	22466021	146.472
	La2	3366021	N3	22466021	66.902
	La2	3366021	Zr11	15556021	125.495
	O2	19456021	Zr2	6466021	144.622
	N3	22466021	Zr11	15556021	162.579
La2	Zr3	7555011	Zr2	6555011	46.610
	Zr3	7555011	La1	2366021	137.766
	Zr3	7555011	N1	20555011	51.896
	Zr3	7555011	N2	21465011	129.414
	Zr3	7555011	O2	19465011	126.029
	Zr3	7555011	N3	22455011	75.341
	La1	2366021	Zr5	9366021	36.613
	Zr6	10555011	Zr8	12555011	47.597
	N1	20555011	Zr5	9366021	122.474
	N2	21465011	O2	19465011	39.792
	N2	21465011	N3	22455011	152.401
	N2	21465011	Zr5	9366021	55.077
	O2	19465011	N3	22455011	118.897
	O2	19465011	Zr5	9366021	54.244
	N3	22455011	Zr5	9366021	99.525
La3	Zr1	5555011	O1	18555011	145.411
	Zr1	5555011	Zr10	14555011	79.278
	Zr6	10555011	Zr12	16555011	78.383
	Zr6	10555011	Zr13	17556021	148.425
Zr1	La3	4555011	Zr6	10555011	67.615
	La3	4555011	Zr10	14555011	58.322
	N2	21456021	Zr13	17556021	96.571
	N2	21456021	Zr12	16466021	107.508
	Zr12	16555011	Zr13	17556021	90.066
	Zr12	16555011	Zr12	16466021	50.934
	Zr13	17556021	Zr12	16466021	136.453
Zr2	Zr3	7555011	Zr6	10555011	30.028
	Zr3	7555011	La2	3555011	56.513
O1	La3	4555011	Bi1	1555011	126.898
	La3	4555011	Zr8	12655011	159.757
	La3	4555011	N3	22555011	131.975
	La3	4555011	Zr12	16555011	66.452
	La3	4555011	Zr13	17555011	127.375
	La3	4555011	Zr7	11555011	95.178
	Bi1	1555011	Zr8	12655011	72.254
	Bi1	1555011	N3	22555011	59.364
	Bi1	1555011	Zr12	16555011	166.607
N1	N3	22455011	Zr3	7555011	117.790
	N3	22455011	Zr8	12555011	80.646
	N3	22455011	Zr4	8555011	147.681
	N3	22455011	N3	22465021	108.028
	N3	22455011	N1	20365021	69.547
	N3	22455011	La2	3555011	89.041
	N3	22455011	Zr2	6555011	135.809
	N3	22455011	La1	2554011	104.767
	N3	22455011	Zr6	10555011	117.167
	N3	22455011	Bi1	1455011	48.004

CONCLUSIONS

In summary, it may be stated that the room temperature crystal structures of three n = 4 Perovskite types of oxides have been refined from high resolution X-ray diffraction data. The pattern decomposition and peak extraction methods have been used for the first time to derive starting models for $Bi_{1.256}$ $La_{0.53}$ $N_{0.231}$ $O_{0.521}$ $Zr_{1.543}$.A model has been proposed for this high temperature phase. It is also confirmed that the ferroelectric to paraelectric phase transition in $Bi_{1.256}$ $La_{0.53}$ $N_{0.231}$ $O_{0.521}$ $Zr_{1.543}$ is not accompanied by a structural phase transition. The zigzag arrangement of the distorted $[ZrO4]^{2-}$ octahedral and LaN is tetrahedral as observed in the n = 2 series of Perovskite phases are found in these structures as well. A rational explanation for the distribution of the Bi/Zr/La cations in the A sites as well as the $[Bi2O2]^{2+}$ sites is provided based on the VBS calculations. $Bi_{1.256}$ $La_{0.53}$ $N_{0.231}$ $O_{0.521}$ $Zr_{1.543}$ shows a structural transition to the prototype triclinic structure in the space group *P-1* at 293K. A model has been proposed for this high temperature phase. It is also confirmed that the ferroelectric to paraelectric phase transition in $Bi_{1.256}$ $La_{0.53}$ $N_{0.231}$ $O_{0.521}$ $Zr_{1.543}$ by a structural phase transition.

REFERENCES

1. Missen, O. P., Kampf, A. R., Mills, S. J., Housley, R. M., Spratt, J., Welch, M. D., ... & Ferraris, C. (2019). The crystal structures of the mixed-valence tellurium oxysalts tlapallite,(Ca, Pb) 3CaCu6 [Te4+ 3Te6+ O12] 2 (Te4+ O3) 2 (SO4) 2· 3H2O, and carlfriesite, CaTe4+ 2Te6+ O8. *Mineralogical Magazine*, *83*(4), 539-549.
2. Brugger, J., Liu, W., Etschmann, B., Mei, Y., Sherman, D. M., & Testemale, D. (2016). A review of the coordination chemistry of hydrothermal systems, or do coordination changes make ore deposits?. *Chemical Geology*, *447*, 219-253.
3. Christy, A. G., & Mills, S. J. (2013). Effect of lone-pair stereoactivity on polyhedral volume and structural flexibility: application to TeIVO6 octahedra. *Acta Crystallographica Section B: Structural Science, Crystal Engineering and Materials*, *69*(5), 446-456.
4. Christy, A. G., Mills, S. J., & Kampf, A. R. (2016). A review of the structural architecture of tellurium oxycompounds. *Mineralogical Magazine*, *80*(3), 415-545.
5. Christy, A. G., Mills, S. J., Kampf, A. R., Housley, R. M., Thorne, B., & Marty, J. (2016). The relationship between mineral composition, crystal structure and paragenetic sequence: the case of secondary Te mineralization at the Bird Nest drift, Otto Mountain, California, USA. *Mineralogical Magazine*, *80*(2), 291-310.
6. Degen, T., Sadki, M., Bron, E., König, U., & Nénert, G. (2014). The highscore suite. *Powder Diffraction*, *29*(S2), S13-S18.
7. Eby, R. K., & Hawthorne, F. C. (1993). Structural relations in copper oxysalt minerals. I. Structural hierarchy. *Acta Crystallographica Section B: Structural Science*, *49*(1), 28-56.
8. Effenberger, H., Zemann, J., & Mayer, H. (1978). Carlfriesite; crystal structure, revision of chemical formula, and synthesis. *American Mineralogist*, *63*(9-10), 847-852.
9. Gagné, O. C., & Hawthorne, F. C. (2015). Comprehensive derivation of bond-valence parameters for ion pairs involving oxygen. *Acta Crystallographica Section B: Structural Science, Crystal Engineering and Materials*, *71*(5), 562-578.
10. Gaines, R. V. (1968). Poughite, a new tellurite mineral from Mexico and Honduras. *American Mineralogist: Journal of Earth and Planetary Materials*, *53*(7-8), 1075-1080.
11. Caskey, C. M., Holder, A., Shulda, S., Christensen, S. T., Diercks, D., Schwartz, C. P., ... & Prendergast, D. (2016). Synthesis of a mixed-valent tin nitride and considerations of its possible crystal structures. *The Journal of chemical physics*, *144*(14), 144201.
12. Bennour, I., Mohamed, M., Kabadou, A., & Abdelmouleh, M. (2020). New perovskite Ba0. 7La0. 3Ti0. 55Fe0. 45O3-δ prepared by citric sol-gel method: From structure to physical properties. *Journal of Molecular Structure*, 128347.
13. Gao, H., Ning, S., Zou, J., Men, S., Zhou, Y., Wang, X., & Kang, X. (2020). The electrocatalytic activity of BaTiO3 nanoparticles towards polysulfides enables high-performance lithium–sulfur batteries. *Journal of Energy Chemistry*, *48*, 208-216.
14. Thanki, A. A., & Goyal, R. K. (2016). Study on effect of cubic-and tetragonal phased BaTiO3 on the electrical and thermal properties of polymeric nanocomposites. *Materials Chemistry and Physics*, *183*, 447-456.
15. Parashuram, M. (2011). Synthesis, crystal structure determination and ionic properties of novel Bi Ca0.5Mg0.5 O2.5 via X- ray powder diffraction data Crystal Growth. 2041 32; 2041-204.
16. Charkin, D. O., Karpov, A. S., Kazakov, S. M., Plokhikh, I. V., Zadoya, A. I., Kuznetsov, A. N., ... & Siidra, O. I. (2019). Synthesis, crystal structure, spectroscopic properties, and thermal behavior of rare-earth oxide selenates, Ln2O2SeO4 (Ln= La, Pr, Nd): The new perspectives of solid-state double-exchange synthesis. *Journal of Solid State Chemistry*, *277*, 163-168.